Specific Neosaxitoxin Interactions with the Na^+ Channel Outer Vestibule Determined by Mutant Cycle Analysis

Jennifer L. Penzotti,* Gregory Lipkind,*,† Harry A. Fozzard,* and Samuel C. Dudley, Jr.‡

Departments of *Neurobiology, Pharmacology, and Physiology and †Biochemistry and Molecular Biology, University of Chicago, Chicago, Illinois 60637; and the ‡Departments of Medicine and Physiology, Emory University, Atlanta, Georgia 30322 and the Atlanta Veterans Administration Medical Center, Decatur, Georgia 30033 USA

ABSTRACT The voltage-gated Na^+ channel α-subunit consists of four homologous domains arranged circumferentially to form the pore. Several neurotoxins, including saxitoxin (STX), block the pore by binding to the outer vestibule of this permeation pathway, which is composed of four pore-forming loops (P-loops), one from each domain. Neosaxitoxin (neoSTX) is a variant of STX that differs only by having an additional hydroxyl group at the N1 position of the 1,2,3 guanidinium (N1-OH). We used this structural variant in mutant cycle experiments to determine interactions of the N1-OH and its guanidinium with the outer vestibule. NeoSTX had a higher affinity for the adult rat skeletal muscle Na^+ channel (μI or Scn4a) than for STX ($\Delta G \sim 1.3$ kcal/mol). Mutant cycle analysis identified groups that potentially interacted with each other. The N1 toxin site interacted most strongly with μI Asp-400 and Tyr-401. The interaction between the N1-OH of neoSTX and Tyr-401 was attractive ($\Delta\Delta G = -1.3 \pm 0.1$ kcal/mol), probably with formation of a hydrogen bond. A second possible attractive interaction to Asp-1532 was identified. There was repulsion between Asp-400 and the N1-OH ($\Delta\Delta G = 1.4 \pm 0.1$ kcal/mol), and kinetic analysis further suggested that the N1-OH was interacting negatively with Asp-400 at the transition state. Changes in pH altered the affinity of neoSTX, as would be expected if the N1-OH site were partially deprotonated. These interactions offer an explanation for most of the difference in blocking efficacy between neoSTX and STX and for the sensitivity of neoSTX to pH. Kinetic analysis suggested significant differences in coupling energies between the transition and the equilibrium, bound states. This is the first report to identify points of interaction between a channel and a non-peptide toxin. This interaction pattern was consistent with previous proposals describing the interactions of STX with the outer vestibule (Lipkind, G. M., and H. A. Fozzard. 1994. *Biophys. J.* 66:1–13; Penzotti, J. L., G. Lipkind, H. A. Fozzard, and S. C. Dudley, Jr. 1998. *Biophys. J.* 75:2647–2657).

INTRODUCTION

The voltage-gated Na^+ channel is the current source for depolarization and conduction of the action potential in most excitable cells of muscle and nerve. The channel is the target of commonly used antiarrhythmic, anticonvulsant, and local anesthetic drugs. A basic property of the channel is its formation of a central pore by circumferential organization of four homologous domains, each with six transmembrane segments. The extracellular loop between the fifth and sixth transmembrane segments of each domain is called the P loop, which folds back into the membrane to form the outer lining of the pore and the selectivity filter (Terlau et al., 1991; Favre et al., 1996; Sun et al., 1997). The asymmetrical marine neurotoxins, STX and tetrodotoxin (TTX), are specific, high-affinity ligands that bind at the Na^+ channel outer vestibule, and the guanidinium groups of each toxin are presumed to inhibit conductance by interacting with the channel selectivity filter (Hille, 1975; Kao and Walker, 1982; Kao, 1986; Kao et al., 1983; Penzotti et al., 1998; Strichartz, 1984). NeoSTX, a naturally occurring variant of STX, is reported to block with higher efficacy (Hu and Kao, 1991; Guo et al., 1987). In comparison to STX, neoSTX differs only by having an additional hydroxyl group at the N1 position of the 1,2,3 guanidinium (Fig. 1). The presence of this hydroxyl group alters the interactions of the N1 site, and it also changes charge distribution on the 1,2,3 guanidinium, affecting any electrostatic interactions of N2 and N3. We used mutant cycle analysis to identify specific residue couplings between the channel and neoSTX with two goals. First, it offered an opportunity to determine the basis of its different blocking efficacy from STX. Second, it was a means of testing our recent model of the STX binding site (Lipkind and Fozzard, 1994; Penzotti et al., 1998).

Establishing specific functional groups involved in coupling between a ligand and its binding site in the absence of structural data has relied most often upon a mutant cycle analysis (Schreiber and Fersht, 1995), and Hidalgo and MacKinnon (1995) were the first to apply this technique to the structural biology of ion channels. This technique requires mutations of both the ligand and the protein binding site of interest. The interdependence of the effect of mutations upon binding efficacy has been taken to suggest points of interaction, and the degree of interdependence has been used to estimate the energy of the interaction. To date, only peptide toxins have been used for that analysis. NeoSTX presented the opportunity to evaluate the utility of mutant cycle analysis using variants of non-peptide ligands. Mutant

Received for publication 22 May 2000 and in final form 16 November 2000.

Address reprint requests to Dr. Samuel C. Dudley, Jr., Assistant Professor of Medicine and Physiology, Division of Cardiology, Emory University/VAMC, 1670 Clairmont Road (111B), Decatur, GA 30033. Tel.: 404-327-4019; Fax: 404-329-2211; E-mail: sdudley@emory.edu.

0006-3495/01/02/698/09 $2.00

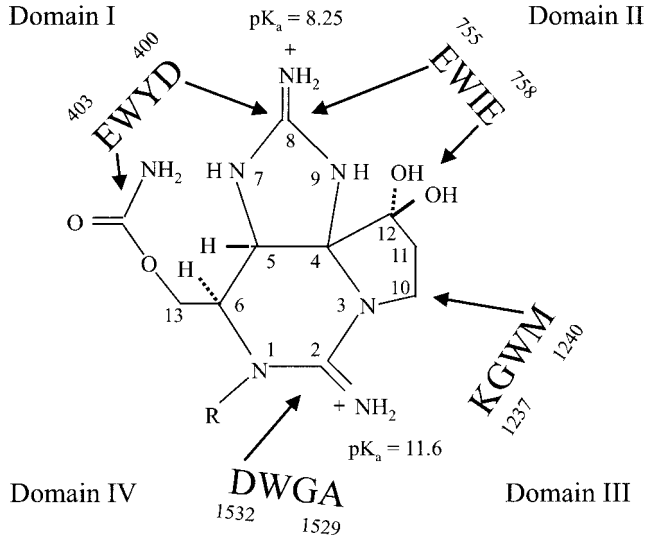

FIGURE 1 The structure of STX (Schantz et al., 1975) and the putative orientations of the carboxyl portion of the four domain P-loops (single-letter amino acid code) with respect to the functional groups of STX as adapted from Lipkind and Fozzard (1994). The principal atoms of STX are numbered in the usual manner, and chiral centers are indicated. NeoSTX has an hydroxyl group substituted for a hydrogen at the N1 position indicated by an R (Shimizu et al., 1978). The domain P-loops are arranged in a clockwise configuration around the toxin as viewed from the extracellular surface. The arrows indicate putative interactions of channel residues with toxin functional groups. The N1-OH group of neoSTX is directed between domains I and IV.

cycle analysis identified interactions of the neoSTX 1-OH, 2,3 guanidinium with channel residues Asp-400, Tyr-401, and possibly Asp-1532. These interactions provide an explanation for the difference in neoSTX and STX affinities. Interactions between the N1-OH ($pK_a \approx 6.75$) and the Asp-400 also provide a possible explanation for some of the striking pH dependence of neoSTX binding in comparison to STX.

MATERIALS AND METHODS

Most methods have been described previously in detail (Penzotti et al., 1998). A brief description emphasizing variations from the previous report is discussed below. Oligonucleotide-directed point mutations were introduced into the adult rat skeletal muscle Na^+ channel (μI or Scn4a). DNA sequencing of the entire polymerized regions ensured that only the intended mutations were present. The vectors were linearized and transcribed with a DNA-dependent RNA polymerase. Stage V and VI *Xenopus* oocytes from female frogs (NASCO, Ft. Atkinson, WI or Xenopus 1, Ann Arbor, MI) were injected with ~50–100 ng of cRNA. Oocytes were incubated at 16° C for 12–72 h before examination.

Recordings were made in the two-electrode voltage clamp configuration. Data were collected using pClamp 6.3 or Axograph 3.5 software (Axon Instruments, Foster City, CA). All recordings were obtained at room temperature (20–22°C). The oocytes were placed in the center of a bath chamber designed to promote laminar flow, and the bath flow was typically 500 μl/min. Previously, we have demonstrated that the solution exchange rate is sufficient to estimate kinetic rate constants. All determinations of blocking efficacy of STX and neoSTX for channel mutants were performed over the same time period and with oocytes injected simultaneously. Wild-type channel toxin binding affinities were reconfirmed periodically to ensure accurate calculation of coupling energies. Some of the STX affinity determinations for μI and all determinations for D400A, E755A, and D1532N were previously reported by Penzotti et al. (1998). Affinity measurements for wild-type channels were reproducible over the experimental period.

The standard bath solution consisted of (in mM): 90 NaCl, 2.5 KCl, 1 $CaCl_2$, 1 $MgCl_2$, and 5 HEPES titrated to pH 7.2 with 1 N NaOH. STX was obtained from Calbiochem (La Jolla, CA), Sigma (St. Louis, MO), or the Marine Analytical Chemistry Standards Program of the Institute of Marine Biosciences, National Research Council of Canada (NRC, Halifax, Nova Scotia) and neoSTX from the NRC. STX from the various sources showed equivalent activity. Stocks were stored at −20°C and showed no degradation over the course of these experiments.

The effect of toxin addition was monitored by recording the peak current elicited every 20 s upon step pulses to 0 mV of 70 ms duration from a holding potential of −100 mV. This protocol allowed the observation of toxin blocking and unblocking, ensured an equilibrium was reached, and avoided the development of use-dependent toxin block. There was no accumulation of inactivated channels with this stimulus rate for the wild-type or mutant channels studied. The IC_{50} for toxin binding was calculated from the ratio of peak currents in the absence and presence of toxin based on a single-site Langmuir absorption isotherm. The change in peak I_{Na} with time was well-fitted by single exponential functions for all combinations of toxins and channel in most experiments, and only those were included in the kinetic analysis. The kinetically derived dissociation constant, K_d, was calculated from the rate constants. When the binding affinity was greater than 1 μM, the toxin concentration was decreased to less than the K_d to clearly resolve the exponential time course for toxin binding, since the on-rate time constant is pseudo-first-order and varies linearly with toxin concentration. Because of their low toxin affinities, kinetic measurements with E755A and D1532N were felt to be affected by the bath exchange rate and were not further analyzed. Time constants were used to calculate rate constants.

The free energy change in toxin binding to a wild-type/mutant channel pair, ΔG, was calculated as the difference of the average $RT\ln(IC_{50})$ for the wild-type and mutant, where R is the gas constant and T is temperature. The standard errors (SE) were estimated as the square root of the variance of the $RT\ln(IC_{50})$ averages divided by the square root of the sum of the number of observations. $\Delta\Delta G$ was taken as the difference of the ΔG values for neoSTX and STX ($\Delta\Delta G = (G_{\mu I,STX} - G_{\mu I,neoSTX}) - (G_{mutant,STX} - G_{mutant,neoSTX})$), and the standard error of this number was reported as the square root of the sum of the variances of the $RT\ln(IC_{50})$ averages (Bevington, 1969) divided by the square root of the sum of the total number of observations minus four. Note that $\Delta\Delta G$ may be positive or negative, both representing a coupling interaction. The negative values represent less coupling energy between the mutant pair as compared to the native residue pair. A positive $\Delta\Delta G$ indicates that the introduced pair has more coupling energy after mutation relative to the native pair. This might occur as a result of relief of a preexisting repulsion or of creating a novel attraction between the new pair. For qualitative assessment of coupling at the transition state, coupling coefficients, Ω, for toxin/channel pairs were calculated as the ratio of the average k_{on} values.

Data are presented as means ± SEM. The number of observations (n) was ≥4 for all reported data except as indicated. Statistical comparisons were performed using two-tailed Student's t-tests assuming unequal variances.

RESULTS

The experimental plan was to use STX and its analog, neoSTX, in combination with wild-type and mutant μI Na^+ channels to determine points of interaction between the N1 STX site on the 1,2,3 guanidinium and residues in the

channel outer vestibule. From this, we could characterize the structural basis of the blocking efficacy difference between STX and neoSTX and could test proposals about the STX/channel interactions. Substitutions of outer vestibule residues previously shown to be important for STX binding were undertaken.

NeoSTX blocked native μI better than STX

Table 1 compares the IC_{50}, k_{on}, k_{off}, and kinetically derived K_d values for STX and neoSTX for the channel mutants tested. There was a good correlation between the equilibrium IC_{50} and the kinetically derived K_d values. As has been shown previously for muscle channels at similar pH values (Guo et al., 1987; Hu and Kao, 1991), neoSTX had a 10-fold higher blocking affinity for the μI Na^+ channel than did STX at a pH of 7.2 ($\Delta G \sim 1.3$ kcal/mol). There is one report noting that STX is slightly more efficacious than neoSTX in blocking μI at pH 7.2 (relative potency: 1.8-fold; Favre et al., 1995). The reason for this difference in the relative blocking efficacies is unclear, but it may be explained by slightly different ionic conditions or differences in the source and purity of neoSTX.

The kinetic K_d value, determined by the average rate constants, for neoSTX was 13-fold smaller than for STX, in agreement with the equilibrium IC_{50} values. The increased affinity of neoSTX was associated with a threefold decrease in the average k_{off} ($p < 0.01$) and a twofold change in the average k_{on} ($p = 0.04$) for neoSTX as compared with STX. These findings are consistent with early reports of neoSTX having a slower dissociation rate than STX (Moczydlowski et al., 1984; Strichartz, 1984). More recently, the relative decrease in k_{off} of neoSTX as compared with STX has been reported to be 5.3 (Guo et al., 1987) and 5.9 (Favre et al., 1995) for reconstituted rat skeletal muscle channels and heterologously expressed μI channels, respectively.

The IC_{50} values of STX and neoSTX for the channel mutants are compared to those for the native channel and plotted in Fig. 2. All mutations decreased the STX and neoSTX blocking efficacies as compared to those of the native channel. The effects of these channel mutations on the IC_{50} values for STX were similar to previous reports (Chen et al., 1997; Favre et al., 1995, 1996; Kontis and Goldin, 1993; Noda et al., 1989; Sun et al., 1997; Terlau et al., 1991). Only one report is available of a mutational effect on neoSTX. Favre et al. (1995) reported an apparent inhibition constant of 275 nM for Y401C, similar to our result of 263 ± 25 nM. Limitations on the supply of neoSTX precluded accurate determination of the IC_{50} values for E403Q and E758Q. At pH 7.2, neoSTX had a higher blocking efficacy than did STX against all channels where a comparison was possible, but the relative differences in STX and neoSTX blocking efficacies were less for the mutation of Tyr-401 and Asp-1532, and greater for Asp-400, than that seen with the native μI channel.

Interactions with Asp-400 and Tyr-401 of domain I at equilibrium

The IC_{50} values were used to calculate coupling energies, $\Delta\Delta G$, between the N1-OH guanidinium toxin site and the outer vestibule residues. Calculation of a significant coupling with Tyr-401 is illustrated in Fig. 3 *A*. The IC_{50} value for block of native channels by STX was 4.1 ± 0.5 nM. The channel mutation, Y401C, caused a 77-fold increase in the STX IC_{50} to 314 ± 13 nM. A similar change was seen with Y401D. If Y401C and the N1-OH group of neoSTX were distant from each other, then the effects of substitutions on the IC_{50} values should have been independent. In other words, the channel mutation should have caused the same 77-fold increase in neoSTX blocking efficacy as it did with STX. This was not the case, however. Y401C caused a

TABLE 1 Comparison of the effects of channel mutations on neoSTX and STX blocking efficacy

Channel Mutation	IC_{50} ± SEM (nM)	*n*	IC_{50} Ratio	k_{on} ± SEM ($nM^{-1}\,s^{-1}$)	*n*	k_{off} ± SEM (s^{-1})	*n*	K_d ± SEM (nM)	*n*
neoSTX									
μI	0.4 ± 0.1	9	1	$8.4 \times 10^{-3} \pm 8.5 \times 10^{-4}$	7	$3.8 \times 10^{-3} \pm 2.3 \times 10^{-4}$	8	0.5 ± 0.1	7
D400A	16.3 ± 1.1	8	41	$4.0 \times 10^{-4} \pm 1.0 \times 10^{-4}$	4	$8.2 \times 10^{-3} \pm 1.1 \times 10^{-3}$	4	24.3 ± 6.3	4
Y401D	106.8 ± 6.2	8	267	$2.4 \times 10^{-5} \pm 4.4 \times 10^{-6}$	7	$5.2 \times 10^{-3} \pm 1.0 \times 10^{-3}$	7	231.9 ± 30.7	7
Y401C	263.4 ± 25.3	8	659	$5.2 \times 10^{-5} \pm 1.0 \times 10^{-5}$	6	$1.4 \times 10^{-2} \pm 2.5 \times 10^{-3}$	6	306.9 ± 64.4	6
E755A	8199.5 ± 989.7	4	20499						
M1240A	1.7 ± 0.1	10	4	$5.5 \times 10^{-3} \pm 1.2 \times 10^{-3}$	10	$1.0 \times 10^{-2} \pm 8.1 \times 10^{-4}$	10	2.4 ± 0.3	10
D1532N	35575.7 ± 2263.6	4	88939						
STX									
μI	4.1 ± 0.5	13	1	$4.3 \times 10^{-3} \pm 1.5 \times 10^{-3}$	8	$1.3 \times 10^{-2} \pm 7.4 \times 10^{-4}$	9	6.3 ± 1.8	8
D400A	1924.9 ± 155.0	10	469	$1.8 \times 10^{-6} \pm 3.3 \times 10^{-7}$	6	$1.0 \times 10^{-2} \pm 1.7 \times 10^{-3}$	6	6524.8 ± 1461.5	6
Y401D	169.3 ± 13.7	10	41	$2.4 \times 10^{-5} \pm 6.2 \times 10^{-6}$	6	$7.1 \times 10^{-3} \pm 5.1 \times 10^{-4}$	6	373.6 ± 73.9	6
Y401C	314.4 ± 12.5	5	77	$6.5 \times 10^{-5} \pm 1.4 \times 10^{-5}$	4	$2.2 \times 10^{-2} \pm 3.4 \times 10^{-3}$	4	376.7 ± 70.6	4
E755A	55035.8 ± 5277.7	8	13423						
M1240A	44.7 ± 3.0	12	11	$5.9 \times 10^{-4} \pm 1.6 \times 10^{-4}$	10	$1.3 \times 10^{-2} \pm 1.6 \times 10^{-3}$	10	29.9 ± 5.6	10
D1532N	127487.2 ± 13078.5	8	31094						

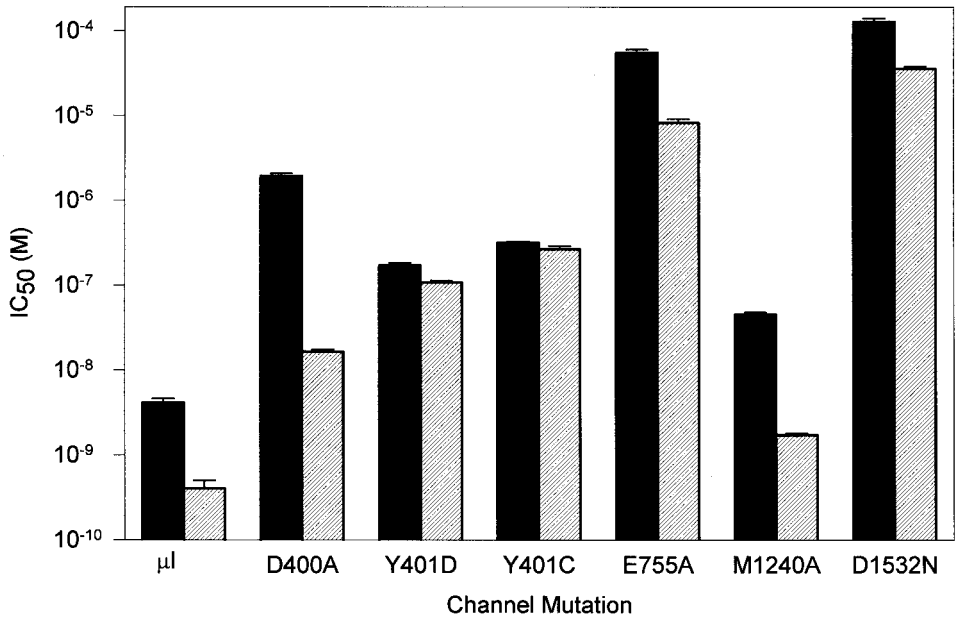

FIGURE 2 Comparison of IC_{50} values of STX (*black bars*) and neoSTX (*striped bars*) for the native μI and seven outer vestibule mutations showing the relative effect of adding the N1-OH group. The differences between the IC_{50} values for STX and neoSTX of the channel mutants as compared to that of native μI suggests couplings between the toxin N1 site and channel residues, Asp-400 and Tyr-401. All experiments were performed at pH 7.2.

658-fold increase in the IC_{50} for neoSTX, a much larger change than predicted. The coupling energy, $\Delta\Delta G$, was -1.3 ± 0.1 kcal/mol ($\Omega = 0.1$), and a similar $\Delta\Delta G$ was seen with Y401D. The considerable coupling energy between Tyr-401 with the N1-OH group establishes an interaction between these two sites, which was hypothesized originally by Moczydlowski and his colleagues (Favre et al., 1995; Guo et al., 1987). Because the cardiac isoform normally has a Cys in this position, it would be expected that there is no difference in STX and neoSTX equilibrium affinities for the heart channel, as reported by Guo et al. (1987). In the presence of STX, the accessibility of sulfhydryl reagents to the cardiac channel outer vestibule is consistent with the lack of a toxin/channel interaction at this site when a Cys is present (Kirsch et al., 1994).

The $\Delta\Delta G$ between the 1,2,3 guanidinium of neoSTX and various channel residues, which is proportional to the logarithm of Ω, is plotted in Fig. 3 *B*. In addition to its strong interaction with Tyr-401, this site appeared to interact with residue Asp-400 of domain I with a $\Delta\Delta G$ of 1.4 ± 0.1 kcal/mol. Mutation of Glu-755, another selectivity filter residue, had a large effect on both STX and neoSTX block, but this effect was independent of the presence of a N1-OH group on the toxin. The addition of the hydroxyl group to position 1 of the 1,2,3 guanidinium group had more modest effects on the change in affinity seen with domain III Met-1240 and domain IV D1532N ($\Delta\Delta G = 0.5 \pm 0.1$ kcal/mol and $\Delta\Delta G = -0.7 \pm 0.1$ kcal/mol, respectively). The small change in STX blocking efficacy seen as a result of M1240A was of similar magnitude to those seen with other neutral mutations of Met-1240 (Pérez-García et al., 1996; Terlau et al., 1991), suggesting that the N1-OH site of STX is probably not interacting strongly with Met-1240 under native conditions.

In summary, comparing the neoSTX/STX IC_{50} ratios for the native channel and the mutants showed that the Tyr-401 formed a strong attractive interaction with the N1-OH guanidinium group of neoSTX, and there was a repulsive force between Asp-400 and the N1-OH.

The transition state interactions differed from those in the equilibrium, bound state

Rate theory predicts that changes in the k_{on} reflect alterations in the transition state energy (Fersht et al., 1992; Matouschek et al., 1989; Penzotti et al., 1998). In combination with mutant cycle analysis, k_{on} values can be used to isolate changes in energy of the transition state as the result of alterations in specific interactions (Chang et al., 1998). Fig. 4 demonstrates the technique used to estimate rate constants and shows the calculation of representative couplings at the transition state. The effect of eliminating the negative charge of Asp-400 by mutagenesis was dependent upon the presence of the N1-OH group, but the changes in k_{on} caused by Y401C were similar in STX or neoSTX. Moreover, a similar small coupling between the N1-OH site and Y401D was observed ($\Omega = 0.4$). The large Ω value for the Asp-400/N1-OH interaction suggested a strong repulsion between the 400 site of the channel and the N1-OH

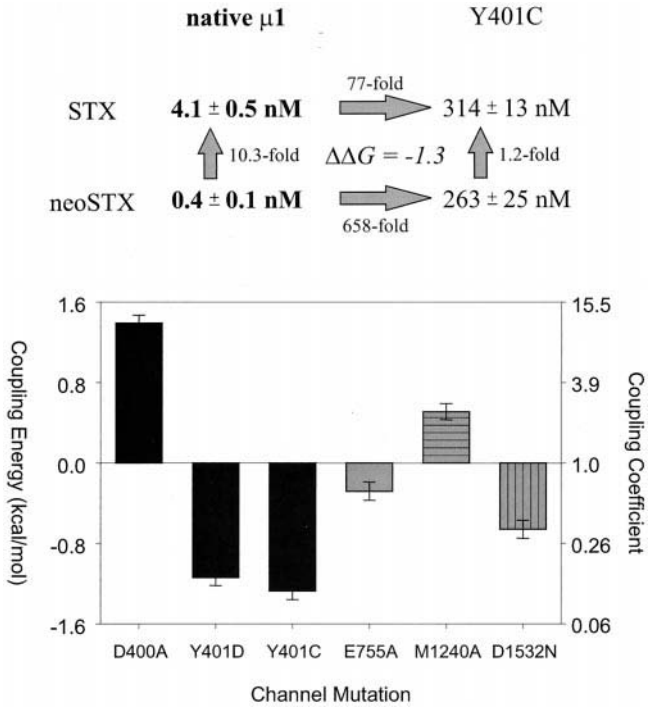

FIGURE 3 (*A*) Calculation of a representative coupling between the Tyr-401 channel site and the toxin N1 site. The channel mutation, Y401C, has a much larger effect on STX blocking efficacy than it does on neoSTX. The dependence of affinity change between toxins on the residue present at the 401 site implies a coupling. (*B*) Coupling energies ($\Delta\Delta G \pm$ SE) between the N1 STX site and outer vestibule residues. The $\Delta\Delta G$ is logarithmically related to the Ω value. Two domain I channel residues, Asp-400 and Tyr-401, show the largest couplings to the 1-OH, 2,3 guanidinium group. Multiple substitutions at the 401 position show that $\Delta\Delta G$ is dependent on the residue substituted. Channel domains I, II, III, and IV are indicated by bars filled with black, gray, horizontal stripes, and vertical stripes, respectively. All experiments were performed at pH 7.2.

guanidinium of STX during association. With alanine present at the 400 site, there was a 222-fold increase in the k_{on} after the N1-OH group was introduced on STX. The cause of this increase was unclear, but with the native aspartate present, no increase in k_{on} was seen with neoSTX. These findings were consistent with a negative interaction between Asp-400 and the N1 site. The large energy of interaction at the transition state compared to the equilibrium, bound state is consistent with a binding process where the initial strong repulsion between Asp-400 and the N1-OH guanidinium is substantially reduced in the equilibrium conformation.

Reduced interaction at the transition state was observed between the toxin N1-OH site and the 401 channel site. The small Ω values at the transition state, but a significant coupling at equilibrium, could be explained if the interaction between Tyr-401 and the N1 site had not formed at the transition state. The observed equivalent decrease in the toxin k_{on} seen with Y401C for both STX and neoSTX must be the result of effects other than that between the N1-OH group and Tyr-401.

NMR experiments have determined that, in free solution, the pK_a of the N1-OH is 6.75 (Shimizu et al., 1978). This abnormally low pK_a for an OH group is thought to be the result of stabilization of the oxyanion by the neighboring 1,2,3 guanidinium group that can alter its positive charge distribution to partially compensate for the deprotonated N1-OH. Under our conditions at pH = 7.2, the N1-OH should have been 76% deprotonated in free solution. Even though the protonation state of the N1-OH group during equilibrium toxin binding with the channel is unclear and though pK_a values can vary considerably as the result of the local environment (Braiman et al., 1996; Chen and Tsien, 1997; Davoodi et al., 1995; Langsetmo et al., 1991; Rousso et al., 1995; Sampogna and Honig, 1994), the observed repulsion between Asp-400 and neoSTX might have been the result of partial deprotonation of the N1-OH at the transition state, and this idea was tested by alteration in the solution pH.

Consistent with this idea, the neoSTX k_{on} values for the wild-type channel increased from 8.4×10^{-3} nM^{-1} s^{-1} ($n = 7$) at pH 7.2 to 1.8×10^{-2} nM^{-1} s^{-1} ($n = 2$) at pH 6.0, a pH favoring N1-OH protonation. This increase was not seen when Asp-400 was neutralized by mutation. With D400A, the k_{on} values were 4.0×10^{-4} nM^{-1} s^{-1} for both pH 7.2 ($n = 4$) and pH 6.0 ($n = 2$), respectively. These changes in the k_{on} are unlikely to be the result of titrating other functional groups on the toxin since the pK_a values of the two guanidinium groups are 8.25 and 11.6 (see Fig. 1; (Kao, 1986; Kao et al., 1983; Shimizu et al., 1975; Shimizu, 1986)). NeoSTX k_{off} values for the wild-type channel were less affected by pH, changing from 3.8×10^{-3} s^{-1} ($n = 8$) at pH 7.2 to 3.4×10^{-3} s^{-1} ($n = 2$) at pH 6.0. At pH 7.2, D400A resulted in only a twofold increase in the neoSTX k_{off} rate, and this effect was not altered by changes in pH. The D400A k_{off} values were 8.2×10^{-3} s^{-1} ($n = 4$) and 5.1×10^{-3} s^{-1} ($n = 2$) at pH 7.2 and 6.0, respectively.

DISCUSSION

NeoSTX has a higher equilibrium affinity for the μI Na^+ channel at pH 7.2 than does STX. The toxin structures differ only by a hydroxyl on N1 of the 1,2,3 guanidinium. This hydroxyl alters the reactivity of the N1 site and also shifts the distribution of positive electrical charge on the guanidinium. The positive charge on N1 favors dissociation of the proton of the hydroxyl, resulting in the unusually low pK_a value of 6.75.

Mutant cycle analysis suggested that the N1-OH of neoSTX was located near P-loop residues of domain I by showing that the N1 site interacted with residues Asp-400 and Tyr-401 of domain I. The presence of the N1-OH improved toxin interactions with Tyr-401 but created repulsion between the toxin and Asp-400. Retention of at least micromolar toxin-blocking efficacy with all channel mutants and the presence of residue-specific couplings argued

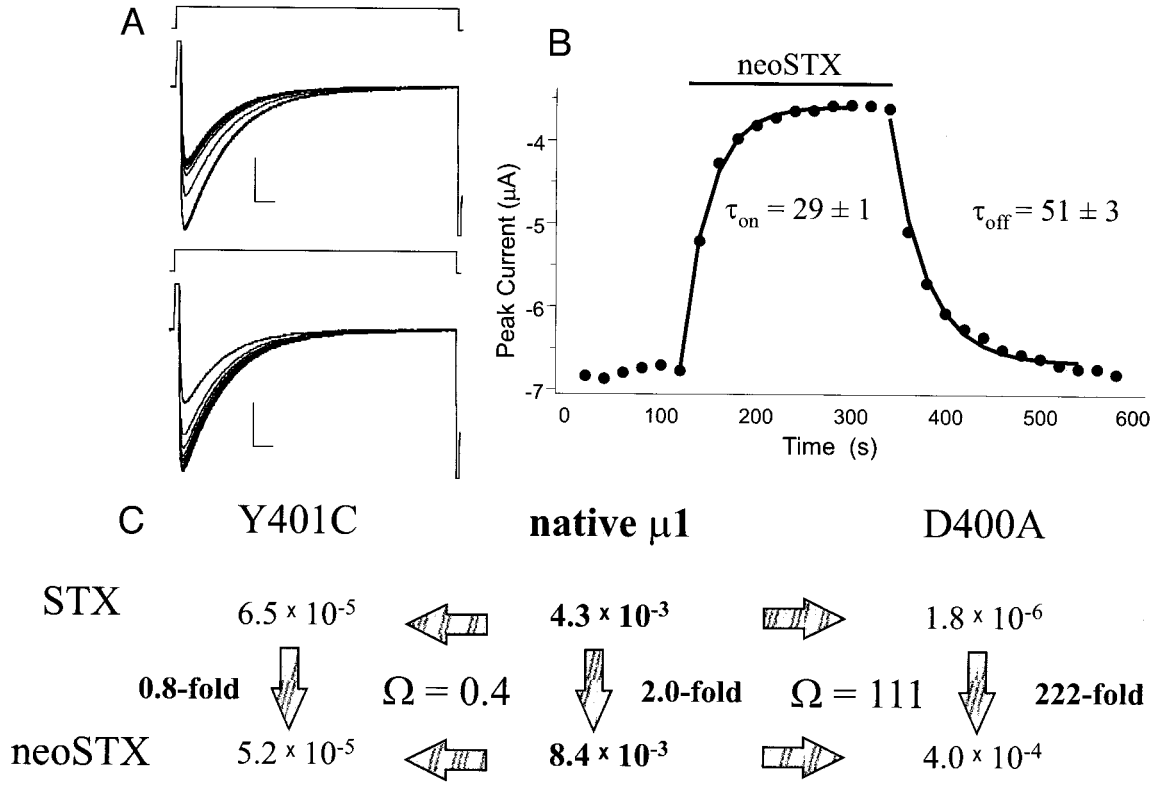

FIGURE 4 Kinetic analysis of toxin/channel interactions at the transition state. (*A*) Current records from an oocyte injected with Y401C. The top family of traces shows the reduction in peak current upon exposure to neoSTX. The bottom traces show recovery of current during washout of the toxin. The square waves indicate timing of the voltage steps from −100 to 0 mV. The calibration bars are 2 μA and 5 ms, respectively. (*B*) Exponential fits to the peak current versus time relationship for the family of currents shown in *A*. Exposure of the channel to 220 nM neoSTX resulted in a 49% reduction in the peak current that fully recovered during washout. The data were well-fitted by single-exponential curves with the time constants shown. (*C*) Mutant cycles showing little coupling between Tyr-401 and the N1 STX site but a significant coupling to Asp-400 during the transition state. Coupling energies at the transition state were considerably different from those at the equilibrium, bound state. The mean k_{on} values are shown for STX and neoSTX for Y401C, native μI, and D400A. All numbers represent the means of four or more independent determinations (pH = 7.2).

against a nonspecific, allosteric explanation for the identified interactions. This is the first report attempting to determine points of interaction between the channel and a non-peptide toxin. These interactions may account for the differences observed in the blocking efficacy of STX and neoSTX.

NeoSTX interactions are consistent with a previous proposal

In 1998, Penzotti et al. proposed a model of STX binding to the Na^+ channel. In that model the 7,8,9 guanidinium group, analogous to the guanidinium of TTX, was directed into the pore, interacting with the selectivity filter Glu-755 of domain II. The 1,2,3 guanidinium group was located at right angles to the plane of the 7,8,9 guanidinium group, with N2 interacting with Asp-1532 of domain IV and N1 in proximity to Tyr-401 (Fig. 5). The data point to an interaction of the N1-OH group with residues in domain I, especially Tyr-401. Based upon the $\Delta\Delta G$ and the fact that Y401F does not change neoSTX affinity (Favre et al., 1995), the Tyr-401/N1-OH interaction seems likely to result from a "hydrogen" bond between the N1-OH and the π electrons of the aromatic ring. Such interactions have been noted before in other proteins (Levitt and Perutz, 1988).

The presence of a hydroxyl at the N1 position provides an experimental marker for the 1,2,3 guanidinium group. The large effect of D1532N on STX binding compared with that of TTX (Penzotti et al., 1998) and the modest coupling of the 1-OH, 2,3 guanidinium site and Asp-1532 ($\Delta\Delta G$ = −07 ± 0.1 kcal/mol), consistent with the modest change in the charge distribution increasing the positive charge on the hydrogen at the N2 site with addition of the N1-OH, provided experimental evidence to support the suggestion that the 1,2,3 guanidinium group is directed toward domain IV. The finding that neoSTX, STX, and TTX were affected equally by mutations of Glu-755 supports the concept that the 7,8,9 guanidinium group, not the 1,2,3 guanidinium group, is directed toward the selectivity filter.

There is a general correspondence between distance separating the 7,8,9 and the 1,2,3 guanidinium groups of neoSTX and the estimated distance separating their pro-

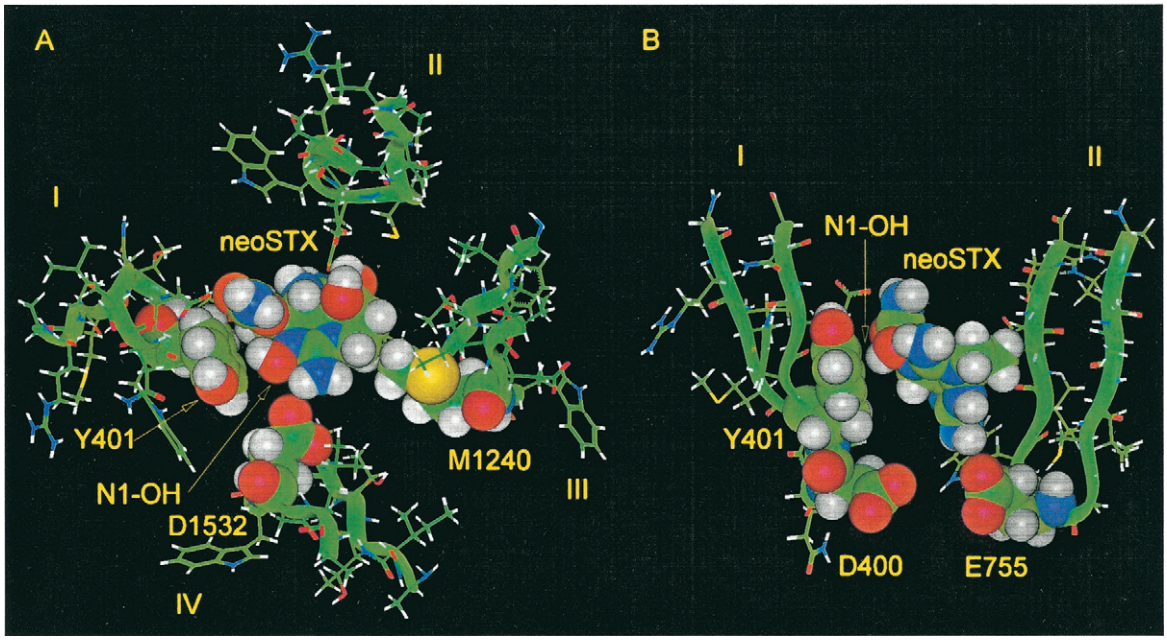

FIGURE 5 A proposed binding arrangement of neoSTX in a model of the μI Na^+ channel outer vestibule adapted from Penzotti et al. (1998). (*A*) The toxin/channel interaction is viewed along the axis of ion permeation and from the extracellular surface. The P-loop carboxy termini from each of the domains are arranged as β-sheets, and their carbon backbones are indicated by green ribbons. The domains are arranged in a clockwise manner such that the N1-OH of neoSTX is closest to domain I, in a position to interact with Asp-400 and Tyr-401. Asp-1532 of domain IV interacts with N2 of the 1,2,3 toxin guanidinium group. (*B*) A side view of the neoSTX/channel interaction emphasizing the proximity of Tyr-401 to the N1-OH. The domain III and IV P-loops have been removed for clarity. Carbon, nitrogen, oxygen, and hydrogen are green, blue, red, and white, respectively.

posed contact points on the channel, Asp-1532, and the selectivity filter, respectively. By systematically introducing Cys residues and determining the accessibility to and electrical depth of Cd^{2+} binding, Tomaselli and his colleagues showed that the pore-forming segments form loops (Chiamvimonvat et al., 1996; Yamagishi et al., 1997). The electrical depth of the Cys-substituted positions increased in a relatively organized fashion with each successive residue from the carboxy terminus until the putative selectivity filter residues were reached (range 3–9%/residue). The electrical distance between Asp-1532 level and the selectivity filter level was ~20% of the field. If the field drop is linear over ~25 Å, then this corresponds to a distance of ~5 Å, a number compatible with the separation of the STX guanidinium groups.

In the model, the Asp-400, Tyr-401, and Asp-1532 interactions were calculated to contribute ~1 kcal/mol to the binding energy of neoSTX as compared with STX, similar to the experimental finding of 1.3 kcal/mol. For this calculation, total energy differences for interactions of the toxins with these three residues were calculated using the cvff force field in the Discover module of Biosym (MSI, Inc., San Diego, CA). Differences in the sum of the $\Delta\Delta G$ values for these three interactions and the ΔG value of STX versus neoSTX binding to the wild-type channel may reflect N1-OH interactions not identified or other factors affecting the determination of coupling energies, such as the dependence of coupling energy on the residue substituted.

Interactions may explain the pH dependence of neoSTX binding

The complex dependency of toxin blocking upon extracellular pH is more marked for neoSTX than for STX (Hu and Kao, 1991; Kao and Walker, 1982; Kao, 1986; Strichartz, 1984). The demonstrated N1-OH/Asp-400 interaction may explain this observation. Lowering the pH causes an increase in the blocking efficacy of neoSTX not seen with STX, and raising the pH causes a larger decrease in affinity of neoSTX than for STX. Several investigators have proposed a repulsion between the deprotonated N1-OH group and a carboxyl group on the channel as the reason for the larger decrease in blocking efficacy of neoSTX than STX at alkaline pH values (Kao, 1986; Strichartz, 1984; Yang et al., 1992). We found evidence for such repulsion between Asp-400 and the N1 site was demonstrated both at the transition state and at the equilibrium, bound state. The reduction in the neoSTX k_{on}, as compared to that of STX, could be eliminated by neutralizing Asp-400, suggesting that a partially deprotonated N1-OH was being repelled by Asp-400 under the control conditions. Alterations in repulsion between the titratable N1-OH and Asp-400 might explain the improved neoSTX binding at reduced pH and the more marked decrease in neoSTX affinity at higher pH.

Nevertheless, the pH dependence is probably more complicated. In our results, there was a strongly positive interaction between the N1-OH of neoSTX and the Tyr-401.

Consistent with the possibility that there is a hydrogen bond between Tyr-401 and the N1-OH group, the improvement of neoSTX blocking efficacy at acidic pH might represent an improved interaction of the protonated N1-OH group with Tyr-401, as previously suggested (Favre et al., 1995; Guo et al., 1987). Changes in the charge distribution at the nitrogens 2 and 3 of the neoSTX guanidinium group as a result of changes in the protonation state of the N1-OH could alter neoSTX interactions with Asp-1532. At the same time, the less positive partial charge on N1 would reduce interaction with Asp-400.

Kinetic analysis suggests significant changes in coupling energies during binding

Comparison of the coupling energies at the transition states and the equilibrium, bound states suggested significant differences in coupling during the binding reaction. At the transition state, there was a strong negative interaction between Asp-400 that was reduced at the equilibrium, bound state. It is tempting to speculate that the reduced repulsion between the N1 site and Asp-400 at equilibrium as compared to the transition state involves increased protonation of the N1 hydroxyl group during binding. It is possible that this protonation occurs because the pH within the vestibule is likely to be lower than that of the solution (Woodhull, 1973; Zhang and Siegelbaum, 1991). This protonation event, presumably after the transition state, would explain the apparent Tyr-401/N1-OH hydrogen bond, the lack of strong coupling between the Tyr-401 and N1 sites until the equilibrium, bound state, and the decreased Asp-400/N1-OH repulsion seen in the equilibrium, bound state as compared with the transition state. The modest positive interaction between the 1,2,3 guanidinium group and Asp-1532 could result from an increased electrostatic interaction, and protonation of N1 would tend to improve this interaction. In any event, the differences observed in coupling energies of a particular residue pair at the transition state and at the equilibrium, bound state give new insight into the reaction coordinate.

In summary, we have compared the effects of Na^+ channel outer vestibule mutations upon the blocking efficacy of STX and its derivative, neoSTX. Through the use of mutant cycle analysis, couplings between the toxin 1,2,3 guanidinium site and channel residues Asp-400, Tyr-401, and possibly Asp-1532 have been identified. Further analysis shows significant differences in interaction energies between the transition and the equilibrium, bound states. The data support aspects of a previous proposal to explain STX interactions with the channel.

Technical assistance was provided by Ian Glaaser, Colleen Parrett, Jon Hall, Junxiu Ling, and Bin Xu. The authors thank Dr. Jack Kyle and Dr. Steven Chang for their assistance.

This research was made possible by an American Heart Association, Southeast Affiliate beginning grant-in-aid (to S.C.D.) and by Program Project Award P01-HL20592 from the National Institutes of Health (to H.A.F.). J.L.P. was a Howard Hughes Medical Institute Medical Student Research Training Fellow. S.C.D. is supported by a Scientist Development Award from the American Heart Association, a Procter and Gamble University Research Exploratory Award, and National Institutes of Health Award HL64828.

REFERENCES

Bevington, P. R. 1969. Propagation of errors. *In* Data Reduction and Error Analysis for the Physical Sciences. P. R. Bevington, editor. McGraw-Hill Book Company, New York. 56–65.

Braiman, M. S., A. K. Dioumaev, and J. R. Lewis. 1996. A large photolysis-induced pK_a increase of the chromophore counterion in bacteriorhodopsin: implications for ion transport mechanisms of retinal proteins. *Biophys. J.* 70:939–947.

Chang, N. S., R. J. French, G. M. Lipkind, H. A. Fozzard, and S. C. Dudley, Jr. 1998. Predominant interactions between μ-conotoxin Arg-13 and the skeletal muscle Na^+ channel localized by mutant cycle analysis. *Biochemistry.* 37:4407–4419.

Chen, S.-F., H. A. Hartmann, and G. E. Kirsch. 1997. Cysteine mapping in the ion selectivity and toxin binding region of the cardiac Na^+ channel pore. *J. Membr. Biol.* 155:11–25.

Chen, X. H., and R. W. Tsien. 1997. Aspartate substitutions establish the concerted action of P-region glutamates in repeats I and III in forming the protonation site of L-type Ca^{2+} channels. *J. Biol. Chem.* 272: 30002–30008.

Chiamvimonvat, N., M. T. Pérez-García, R. Ranjan, E. Marban, and G. F. Tomaselli. 1996. Depth asymmetries of the pore-lining segments of the Na^+ channel revealed by cysteine mutagenesis. *Neuron.* 16:1037–1047.

Davoodi, J., W. W. Wakarchuk, R. L. Campbell, P. R. Carey, and W. K. Surewicz. 1995. Abnormally high pK_a of an active-site glutamic acid residue in *Bacillus circulans* xylanase. The role of electrostatic interactions. *Eur. J. Biochem.* 232:839–843.

Favre, I., E. Moczydlowski, and L. Schild. 1995. Specificity for block by saxitoxin and divalent cations at a residue which determines sensitivity of sodium channel subtypes to guanidinium toxins. *J. Gen. Physiol.* 106:203–229.

Favre, I., E. Moczydlowski, and L. Schild. 1996. On the structural basis for ionic selectivity among Na^+, K^+, and Ca^{2+} in the voltage-gated sodium channel. *Biophys. J.* 71:3110–3125.

Fersht, A. R., A. Matouschek, and L. Serrano. 1992. I. Theory of protein engineering analysis of stability and pathway of protein folding. *J. Mol. Biol.* 224:771–782.

Guo, Z., A. Uehara, A. Ravindran, S. H. Bryant, S. Hall, and E. Moczydlowski. 1987. Kinetic basis for insensitivity to tetrodotoxin and saxitoxin in sodium channels of canine heart and denervated rat skeletal muscle. *Biochemistry.* 26:7346–7556.

Hidalgo, P., and R. MacKinnon. 1995. Revealing the architecture of a K^+ channel pore through mutant cycles with a peptide inhibitor. *Science.* 268:307–310.

Hille, B. 1975. The receptor for tetrodotoxin and saxitoxin. A structural hypothesis. *Biophys. J.* 15:615–619.

Hu, S. L., and C. Y. Kao. 1991. Interactions of neosaxitoxin with the sodium channel of the frog skeletal muscle fiber. *J. Gen. Physiol.* 97:561–578.

Kao, C. Y. 1986. Structure-activity relations of tetrodotoxin, saxitoxin and analogues. *Ann. N.Y. Acad. Sci.* 479:52–67.

Kao, P., M. James-Kracke, and C. Kao. 1983. The active guanidinium group of saxitoxin and neosaxitoxin identified by the effects of pH on their activities on squid axon. *Pflügers Arch.* 398:199–203.

Kao, C. Y., and S. E. Walker. 1982. Active groups of saxitoxin and tetrodotoxin as deduced from action of saxitoxin analogs on frog muscle and squid axon. *J. Physiol. (Lond.).* 323:619–637.

Kirsch, G. E., M. Alam, and H. A. Hartmann. 1994. Differential effects of sulfhydryl reagents on saxitoxin and tetrodotoxin block of voltage-dependent Na channels. *Biophys. J.* 67:2305–2315.

Kontis, K. J., and A. L. Goldin. 1993. Site-directed mutagenesis of the putative pore region of the rat IIA sodium channel. *Mol. Pharmacol.* 43:635–644.

Langsetmo, K., J. A. Fuchs, and C. Woodward. 1991. The conserved, buried aspartic acid in oxidized *Escherichia coli* thioredoxin has a pK_a of 7.5. Its titration produces a related shift in global stability. *Biochemistry.* 30:7603–7609.

Levitt, M., and M. F. Perutz. 1988. Aromatic rings act as hydrogen bond acceptors. *J. Mol. Biol.* 201:751–754.

Lipkind, G. M., and H. A. Fozzard. 1994. A structural model of the tetrodotoxin and saxitoxin binding site of the Na^+ channel. *Biophys. J.* 66:1–13.

Matouschek, A., J. Kellis, L. Serrano, and A. R. Fersht. 1989. Mapping the transition state and pathway of protein folding by protein engineering. *Nature.* 340:122–126.

Moczydlowski, E., S. Hall, S. S. Garber, G. S. Strichartz, and C. Miller. 1984. Voltage-dependent blockade of muscle Na^+ channels by guanidinium toxins. Effects of toxin charge. *J. Gen. Physiol.* 84:687–704.

Noda, M., H. Suzuki, S. Numa, and W. Stühmer. 1989. A single point mutation confers tetrodotoxin and saxitoxin insensitivity on the sodium channel-II. *FEBS Lett.* 259:213–216.

Penzotti, J. L., G. Lipkind, H. A. Fozzard, and S. C. Dudley, Jr. 1998. Differences in saxitoxin and tetrodotoxin binding revealed by mutagenesis of the Na^+ channel outer vestibule. *Biophys. J.* 75:2647–2657.

Pérez-García, M. T., N. Chiamvimonvat, E. Marban, and G. F. Tomaselli. 1996. Structure of the sodium channel pore revealed by serial cysteine mutagenesis. *Proc. Natl. Acad. Sci. U.S.A.* 93:300–304.

Rousso, I., N. Friedman, M. Sheves, and M. Ottolenghi. 1995. pK_a of the protonated Schiff base and aspartic 85 in the bacteriorhodopsin binding site is controlled by a specific geometry between the two residues. *Biochemistry.* 34:12059–12065.

Sampogna, R. V., and B. Honig. 1994. Environmental effects on the protonation states of active site residues in bacteriorhodopsin. *Biophys. J.* 66:1341–1352.

Schantz, E. J., V. E. Ghazarossian, H. K. Schnoes, F. M. Strong, J. P. Springer, J. O. Pezzanite, and J. Clardy. 1975. The structure of saxitoxin. *J. Am. Chem. Soc.* 97:1238.

Schreiber, G., and A. R. Fersht. 1995. Energetics of protein-protein interactions: analysis of the Barnase-Barstar interface by single mutations and double mutant cycles. *J. Mol. Biol.* 248:478–486.

Shimizu, Y. 1986. Chemistry and biochemistry of saxitoxin analogues and tetrodotoxin. *Ann. N.Y. Acad. Sci.* 479:24–31.

Shimizu, Y., M. Alam, Y. Oshima, and W. E. Fallon. 1975. Presence of four toxins in red tide infested clams and cultured *Gonyaulax tamarensis* cells. *Biochem. Biophys. Res. Commun.* 66:731–737.

Shimizu, Y., C. P. Hsu, W. E. Fallon, Y. Oshima, I. Miura, and K. Nakanishi. 1978. Structure of neosaxitoxin. *J. Am. Chem. Soc.* 100: 6791–6793.

Strichartz, G. 1984. Structural determinants of the affinity of saxitoxin for neuronal sodium channels. *J. Gen. Physiol.* 84:281–305.

Sun, Y. M., I. Favre, L. Schild, and E. Moczydlowski. 1997. On the structural basis for size-selective permeation of organic cations through the voltage-gated sodium channel. Effect of alanine mutations at the DEKA locus on selectivity, inhibition by Ca^{2+} and H^+, and molecular sieving. *J. Gen. Physiol.* 110:693–715.

Terlau, H., S. H. Heinemann, W. Stühmer, M. Pusch, F. Conti, K. Imoto, and S. Numa. 1991. Mapping the site of block by tetrodotoxin and saxitoxin of sodium channel-II. *FEBS Lett.* 293:93–96.

Woodhull, A. M. 1973. Ionic blockage of sodium channels in nerve. *J. Gen. Physiol.* 61:687–708.

Yamagishi, T., M. Janecki, E. Marban, and G. F. Tomaselli. 1997. Topology of the P segments in the sodium channel pore revealed by cysteine mutagenesis. *Biophys. J.* 73:195–204.

Yang, L., C. Kao, and Y. Oshima. 1992. Actions of decarbamoyloxsaxitoxin and decarbamoylneosaxitoxin on the frog skeletal muscle fiber. *Toxicon.* 30:645–652.

Zhang, J. F., and S. A. Siegelbaum. 1991. Effects of external protons on single cardiac sodium channels from guinea pig ventricular myocytes. *J. Gen. Physiol.* 98:1065–1083.